culation used to produce the simulations is little more than a rearrangement of a simple quantum mechanical formula. It gives the distance (in angstroms) at which a tunneling reaction may occur within time t (in seconds) (*2, 3, 6*) as:

$$a = a_0 + 2.26(15 + \log t)\, B^{-1/2} \quad (2)$$

where B is the binding energy (in electron volts) required to remove the electron from the electron donor ϕ_2^-, and a_0 corrects for the finite radii of ϕ_2^- and ϕ_3Et (a_0 is taken to be 5 Å).

Because the tunneling rate changes by a factor of 10 for each 1.8-Å change in distance, the electron will be transferred from ϕ_2^- to the nearest ϕ_3Et (*3*). If ϕ_2^- is randomly distributed relative to ϕ_3Et, then the fraction of the ϕ_2^- which survives reaction is (*3*)

$$P = \exp(-2.51 \times 10^{-3}\, a^3\, M) \quad (3)$$

where M is the molar concentration, and a increases with time according to Eq. 2. For the calculated curves given in Fig. 1, B was taken to be 1.6 ev, which is the photon energy necessary to photodetach electrons from ϕ_2^- in a hydrocarbon matrix (*3*).

An efficiency factor was introduced as an adjustable parameter since the observed reactions were slightly slower than the calculation. This factor could be considered to represent the slowing of the reaction as a result of Franck-Condon restrictions. This efficiency factor, taken to be $10^{-1.5}$, affected the calculated curves by simply translating them 1.5 units along the log t axis in Fig. 1. This efficiency factor, the only adjustable parameter in the calculation, could have been omitted and a similar fit to the data obtained, if the binding energy were treated as an adjustable parameter.

The kinetics of the observed reactions are very unusual but are in accord with the predictions of a simple model of electron tunneling. The frozen ethanol matrix is known to trap reactive species such as solvated electrons indefinitely (for days at least). This and the unusual kinetics tend to rule out any diffusion mechanism. At the ϕ_3Et concentrations of 0.10M, 0.03M, and 0.01M, the average distances from a ϕ_2^- to the *nearest* ϕ_3Et are 14, 21, and 30 Å, respectively, on the assumption of a random distribution. These and other results (*1–3, 5, 6*) point strongly toward a reaction mechanism in which electrons tunnel through tens of angstroms of inert matrix.

The simple model applied here works reasonably well, but why it works is not known. An appropriate theory must treat not only the electronic and nuclear states of the electron donor and acceptor molecules but also those of the intervening solvent. Approaches to at least part of this problem are being worked out in theories which describe electron transfer reactions in solution as tunneling processes by the use of modern radiationless transition theory (*10*).

JOHN R. MILLER

Chemistry Division, Argonne National Laboratory, Argonne, Illinois 60439

References and Notes

1. B. G. Ershov and E. L. Tseitlin, *Khim. Vys. Energ.* **4**, 186 (1970); F. Kieffer, C. Meyer, J. Rigant, *Chem. Phys. Lett.* **11**, 359 (1971); K. I. Zamaraev, R. F. Khairutidov, A. I. Mikhailov, V. I. Goldanskii, *Dokl. Akad. Nauk SSSR* **199**, 640 (1971); J. Kroh and C. Stradowski, *Int. J. Radiat. Phys. Chem.* **5**, 243 (1973).
2. A. I. Mikhailov, *Dokl. Akad. Nauk SSSR* **197**, 136 (1971).
3. J. R. Miller, *J. Chem. Phys.* **56**, 5173 (1971).
4. A. Habersbergerova, *Radiat. Res. Rev.* **4**, 123 (1972); N. Christodouleas and W. Hamill, *J. Am. Chem. Soc.* **86**, 5413 (1964).
5. D. DeVault and B. Chance, *Biophys. J.* **6**, 825 (1966); D. DeVault, J. Parkes, B. Chance, *Nature (Lond.)* **215**, 642 (1967); J. D. McElroy, D. C. Mauzerall, G. Feher, *Biochim. Biophys. Acta* **333**, 261 (1974).
6. J. Miller, *Chem. Phys. Lett.* **22**, 180 (1973).
7. A. K. Pikaev, *The Solvated Electron in Radiation Chemistry* [Israel Program for Scientific Translations, Jerusalem (available from the U.S. National Technical Information Service, Springfield, Va.), 1973].
8. R. M. Hochstrasser and M. Kasha, *Photochem. Photobiol.* **3**, 317 (1964).
9. R. Foster, *Organic Charge-Transfer Complexes* (Academic Press, New York, 1969), p. 297.
10. For recent examples with several references, see: S. F. Fisher, *Chem. Phys.* **5**, 183 (1974); N. R. Kestner, J. Logan, J. Jortner, *J. Phys. Chem.* **78**, 2148 (1974).
11. Based on work performed under the auspices of the U.S. Atomic Energy Commission.

25 September 1974; revised 21 March 1975

Hammondia hammondi: A New Coccidium of Cats Producing Cysts in Muscle of Other Mammals

Abstract. *Predominant muscle parasitism, and an obligatory two-host cycle (cat-mouse-cat), distinguishes an otherwise similar organism from* Toxoplasma. *The presence of multiplicative stages in the cat gut separate it from* Sarcocystis. *Antibody that cross reacts with* Toxoplasma *antigen is developed in mice and other experimental intermediary hosts, but not in cats, the final host. Recognition of the two-host cycle is essential for the experimental isolation and transmission of the parasite, and for prevention of the infection.*

We isolated an organism from a cat (CR-4) which showed similarities to both *Toxoplasma* and *Sarcocystis*, but which was significantly different from either. Oocysts resembling those of *Toxoplasma* appeared in the feces of an adult feral cat that had been injected with an immunosuppressive corticosteroid. Mice injected with oocysts developed low titers of *Toxoplasma* antibody without evidence of lesions in viscera and brain, but with cysts in skeletal muscle. Although the cysts contained organisms resembling *Toxoplasma*, they were not infectious to other mice. Cysts were infectious to cats which, however, failed to develop antibody to *Toxoplasma*.

We made a systematic comparison with the M-7741 strain of *Toxoplasma*, using techniques in mice and cats as described (*1*).

Oocysts shed by cats were subspherical to spherical, measuring 10.6 by 11.4 μm (10.5 to 12.5 by 11.2 to 13.2 μm). The oocyst wall was colorless, about 0.5 μm in thickness, and consisted of two layers. A micropyle and polar granules were absent. The sporont was uniformly granular and filled about 90 percent of the optical cross section of the oocyst.

Sporulation of oocysts was complete at 72 hours at 20° to 23°C, with two sporocysts containing four sporozoites each. The sporulated oocyst was subspherical to ellipsoidal, measuring 10.6 by 13.2 μm (10.0 to 10.7 by 12.6 to 13.8 μm). There was no oocyst residuum (Fig. 1A).

Sporocysts measured 6.5 by 9.8 μm (6.0 to 7.5 by 8.0 to 10.7 μm). There was no Stieda body. The sporocyst residuum consisted of granules, either dispersed or compact, near the center of the sporocyst. The sporozoites were elongate and slightly curved, measuring approximately 2 by 7 μm; the nucleus was centrally placed.

In mice infected with sporulated oocysts, organisms multiplied initially in the gut wall and mesenteric lymph nodes. After 11 to 16 days, cysts were seen in sections of skeletal muscle and cardiac muscle; after 20 to 48 days in fresh spreads of abdominal wall and diaphragm (Fig. 1, B and C). This was accompanied by necrosis, myositis, and myocarditis.

Cysts gradually increased in size to about 90 by 340 μm and persisted for at least 500 days in the skeletal muscle of mice. Cysts in heart muscle were few and rarely exceeded 30 μm in length. Cysts in brain tissue were rare, spherical in configuration, and measured up to 70 μm in diameter.

Bradyzoites, slowly multiplying organisms within the cysts, were slender, measuring about 2 by 7 μm, and resembled *Toxoplasma*. They differed from the broad and stubby bradyzoites of *Sarcocystis*.

In cats infected with skeletal muscle of

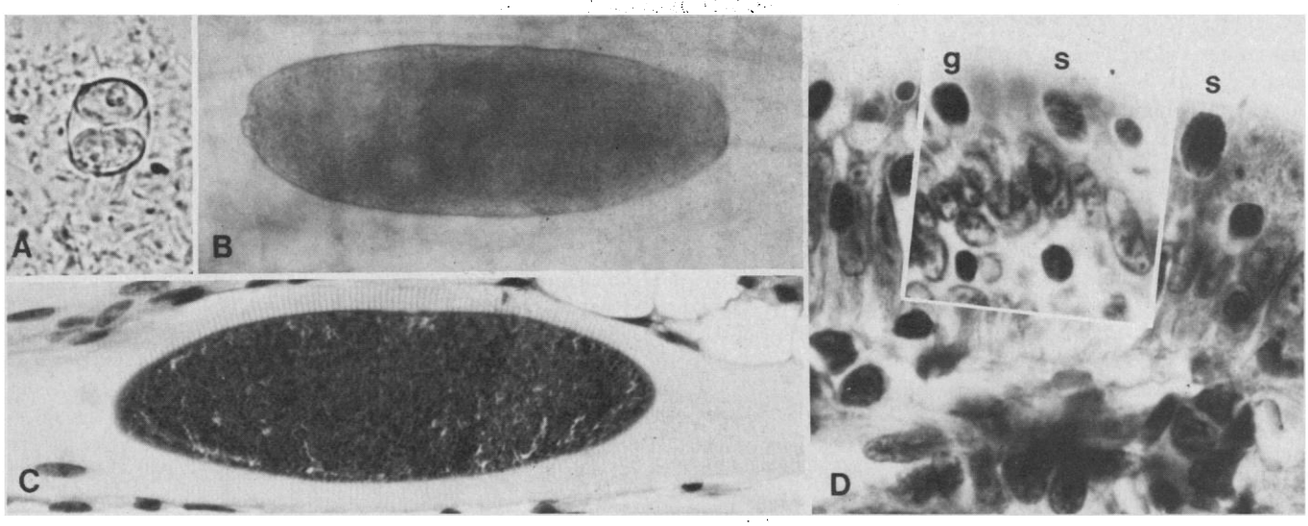

Fig. 1. *Hammondia hammondi.* (A) Sporulated oocyst from cat. The sporocyst residual granules are not sharp due to Brownian movement (×1000). (B) Unstained cyst in skeletal muscle of mouse (×275). (C) Cyst stained with PASH (×400). (D) Multiplicative stages and young gametocytes in the intestinal epithelium of a cat (×1000); *s*, schizont; *g*, gametocyte.

mice containing cysts, schizonts resembling those of *Toxoplasma* types D-ii and E (*1*) were seen in epithelial cells of villi and glands of the jejunum after 4 to 6 days (Fig. 1D). Gametocytes were present between days 5 and 10; oocyst shedding normally started after 5 and 6 days, and continued for 12 to 28 days.

Cats are the *final host* since they support the sexual cycle, and mice are *intermediate hosts* since they do not. An obligatory host change between final and intermediate hosts was necessary for transmission to take place (Fig. 2). Cats could be regularly infected with muscle cysts from mice, as shown by oocyst shedding in 29 of 30 cats. However, none of 16 cats shed oocysts when fed 10^4 to 10^6 oocysts. Mice could be regularly infected with 10 to 100 oocysts, as shown by the development of cysts in muscle. However, mice could not be infected with cysts or tachyzoites from other mice; the carcasses of six cyst-inoculated mice were fed to three cats, which failed to shed oocysts during a 20-day observation period and proved nonimmune when challenged directly with cysts.

Immunity in cats to the homologous infection was pronounced, with 13 of 14 cats failing to again shed oocysts. However, cats immune to the new parasite could be reinfected with *Toxoplasma* and vice versa.

Cross-immunity was seen in mice between *Toxoplasma* and the new parasite. Of groups of mice immunized with 10^5 oocysts of the new parasite, six out of six resisted challenge with 10^3 *Toxoplasma*, five of six resisted challenge with 10^4, and four of six resisted 10^5 *Toxoplasma* oocysts; in comparison, a dose of 10^2 was fatal to six of six normal mice. In 13 mice immune to *Toxoplasma* and challenged with the new parasite, one muscle cyst was found, whereas 22 muscle cysts were found in a comparable number of nonimmune mice.

Antibody to *Toxoplasma* developed in mice infected with the new organism when fed 10^3 or more oocysts. After 3 months, dye test titers of 1:16 to 1:48 were observed. By contrast, *Toxoplasma*-infected mice had titers of 1:1024 or higher. However, no *Toxoplasma* antibody was found in 14 cats that had shed the new oocysts after being fed muscle cysts from mice.

Rats, hamsters, guinea pigs, white-footed mice (*Peromyscus*), and multimammate rats (*Mastomys*) could be infected with oocysts as judged by an antibody response. The first three species, when fed to cats, initiated oocyst shedding. Pigeons could not be so infected.

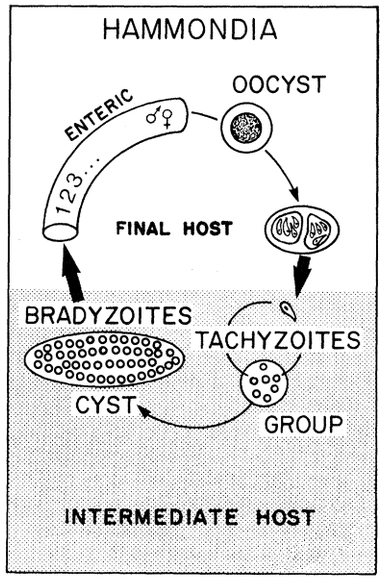

Fig. 2. Obligatory two-host cycle of *Hammondia hammondi.* Unlike *Isospora* and *Toxoplasma*, the oocysts are not infectious to final hosts. Unlike *Toxoplasma*, the bradyzoites are not infectious to the intermediate hosts. Unlike the known *Sarcocystis* species, multiplicative stages precede the development of gametocytes in the intestinal epithelium, and oocysts are shed unsporulated.

We designated the new organism *Hammondia hammondi*, in memory and in honor of the late Professor Datus M. Hammond, who by his research, training of others, and editorial efforts contributed much to our knowledge of the coccidia (*2*).

Hammondia genus is a member of the family Sarcocystidae [Apicomplexa: Coccidiasina: Eimeriorina, according to Levine (*3*)], which is described as obligatorily heteroxenous, forming intracellular cysts in striated muscle (*2*). The genus typically forms elongate cysts in skeletal muscle, with rare subspherical cysts in brain and perhaps elsewhere. Cysts are without septa or radial spines (as found in the genus *Sarcocystis*). Bradyzoites are slender as in *Toxoplasma*. Multiplicative stages precede sexual stages in the intestine of carnivores. The oocysts are shed unsporulated, with sporogony outside of the host resulting in two sporocysts, each with four sporozoites.

Hammondia hammondi, as shed in feces of cats, the final host, has oocysts averaging 10 by 13 μm. The prepatent period to oocyst shedding is 5 to 8 days. Experimental intermediary hosts are laboratory mice, rats, hamsters, guinea pigs, and white-footed mice, in which muscle cysts are formed. The type isolate, CR-4, came from a chronically infected feral cat from Weldon, southern Iowa. A similar organism, WC-1170, A-cyst, was identified from a cat in Oahu, Hawaii (*4*), based on reciprocal cross-immunity tests in cats.

Hammondia hammondi differs from *Toxoplasma gondii* by noninfectivity of

tachyzoites and bradyzoites to other intermediate hosts, and by noninfectivity of oocysts to nonimmune final hosts. While parasitism of skeletal muscle is a pronounced feature of the new genus *Hammondia*, it differs from *Sarcocystis*, the classical muscle parasite, by slender bradyzoites, thin-walled cysts, absent radial spines, septa, or metrocytes, by a multiplicative cycle in the gut of the final host (which is lacking in all *Sarcocystis* so far studied), and by shedding of unsporulated oocysts (whereas all known *Sarcocystis* shed sporulated sporocysts or oocysts).

The new genus differs from the common *Isospora* of cats, which are typically one-host parasites, with the oocyst infectious to the final host. However, an isosporan of dogs studied by Heydorn (*5*) is probably a species of *Hammondia*, since the oocysts were not infectious to dogs, whereas muscles of infected calves did infect dogs.

Hammondia hammondi is the first organism described which produces cross-reacting antibody to *Toxoplasma gondii* in the dye test. This could lead to a mistaken diagnosis of *Toxoplasma* infection in animals. It is not known whether humans become infected with *Hammondia*; however, morphologically compatible cysts have been observed by one of us (J.K.F.).

Recognition of an isolate of *Hammondia* could be delayed by misinterpreting the *Toxoplasma* antibody titer in the intermediate host. The isolate could be lost if tissue cysts were subinoculated from one to another intermediate host instead of to a final host which may be unknown. Prevention of the infection depends also on knowledge of the two-host cycle.

J. K. FRENKEL
J. P. DUBEY*
Department of Pathology and Oncology, University of Kansas Medical Center, Kansas City 66103

References and Notes

1. J. P. Dubey and J. K. Frenkel, *J. Protozool.* **19**, 155 (1[illegible] → *J. Parasitol.* **59**, 505 (1973).
2. J. K. Fenkel, *Z. Parasitenkd.* **45**, 125 (1974); _____ → J. P. Dubey, *ibid.* **46**, 3 (1975).
3. N. D. Levine, in *The Coccidia: Eimeria, Isospora, Toxoplasma, and Related Genera*, D. M. Hammond and P. L. Long, Eds. (University Park Press, Baltimore, 1973), p. 1.
4. G. D. Wallace, *Science* **180**, 1375 (1973); *Z. Parasitenkd.*, in press.
5. A.-O. Heydorn, *Berl. Munch. Tierarztl. Wochenschr.* **86**, 323 (1973).
6. Supported by NIH grant AI-07489.
* Present address: Department of Veterinary Pathobiology, College of Veterinary Medicine, Ohio State University, Columbus 43210.

25 November 1974; revised 16 January 1975

Superior Colliculus: Visuotopic-Somatotopic Overlap

Abstract. *A laminar organization was present in the superior colliculus of the cat, with upper layer cells exclusively visual, lower layer cells primarily somatic (or acoustic), and intermediate layers showing significant modality overlap. The close topographic correspondence between the visual and somatic representations observed within this laminar pattern and the similarities in visual and somatic response specificity may be consistent with the hypothesis that the colliculus combines several sensory modalities to facilitate tracking of a given stimulus.*

The nature of the profound visual deficits appearing after superior colliculus destruction in the cat has led to suggestions that it is involved in visually guided (orienting and following) behavior (*1, 2*). Although relatively little is known about the properties of nonvisual cells in the superior colliculus, the colliculus is known to receive somatic and acoustic afferents in addition to visual projections (*3*). The developmental chronology of sensory representation in the cat superior colliculus has been shown to parallel the animal's use of modality-specific cues for tracking behavior (*4, 5*). Somatic stimuli are effective in activating superior colliculus cells at birth, when orientation is accomplished by means of somatic cues, while acoustic followed by visual activation develops many days later (*4*) along with auditory and visual orientation behavior. These observations, coupled with evidence that colliculus lesions induce somatic and auditory localization deficits (although less profound than visual consequences) (*1*), make it seem reasonable to suppose that just as the visual cells of the colliculus are involved in visual tracking behavior, somatic and acoustic cells are involved in somatic and auditory tracking behavior. In the present experiments we studied the location, organization, and specificity of tactile cells in the colliculus to determine whether the properties of these cells are consistent with this hypothesis. An abstract of this work has been presented (*6*).

Experiments were performed on 30 immobilized (*7*) and artificially respired cats. Animals were surgically prepared for recording with halothane anesthesia, and mixtures of 70 to 75 percent nitrous oxide and 25 to 30 percent oxygen were given during recording sessions. Visual receptive fields of superior colliculus cells were used as referents to which tactile receptive fields could be related. The pupils were dilated with 1 percent atropine, and the locations of the optic discs were determined with an ophthalmoscope and projected onto a transparent hemisphere used for mapping visual fields. Contact lenses focused the eyes on the hemisphere, and body temperature was maintained at 36 ± 2°C by a circulating hot water pad. When each experiment was terminated, intravenous pentobarbital sodium (40 mg per kilogram of body weight) was administered and the animal was perfused through the heart with saline followed by 10 percent formalin. The brain was sectioned at 15-μm thickness and stained with cresyl violet for histological reconstruction of electrode tracks.

Electrodes were vertically oriented. As an electrode was advanced through the laminae of the superior colliculus, natural visual, tactile, and acoustic stimuli (*8*) were delivered continuously. The upper layers of the colliculus proved to be exclusively visual (*9*); cells activated by tactile stimulation (N = 220) as well as acoustic cells were not encountered until the electrode reached the stratum griseum intermediale, where multimodal cells, which have been previously described (*10–12*), were also encountered. As the electrode advanced into the stratum profundum, the incidence of visually activated cells diminished markedly. A basic pattern emerged, with the upper layers strictly visual, the lower layers primarily nonvisual, and the intermediate layers representing a zone of "modality overlap."

Although tactile receptive fields ranged from a few millimeters in extent (primarily on the contralateral forepaw and face) to more than half the contralateral cutaneous surface, the organization was distinctly somatotopic. The presence of a well-ordered visuotopy in upper layer cells (*11, 13, 14*) enabled us to compare the spatial organization of the two modalities. This was accomplished by first mapping the contralateral visual fields of one to four single cells, or a multiunit group, in each of 85 electrode penetrations. The center of the group of receptive fields of each penetration was then used as the visual "reference point" to which the lower layer tactile receptive fields of that penetration were referred (Fig. 1).

In those penetrations in which the visual reference points were near the area centralis, tactile receptive fields were centered toward the midline of the face, near the nose. This is illustrated in the example of a reconstructed electrode penetration in Fig. 1. As the visual fields moved away from the area centralis, tactile fields also moved away from the nose in corresponding directions; for instance, penetrations in which visual reference points were immedi-